(revised 3/9/07)

rf SQUID

Advanced Laboratory, Physics 407
University of Wisconsin
Madison, Wisconsin 53706

Abstract

The Superconducting QUantum Interference Device (SQUID) is the most sensitive detector of magnetic flux available. A Nb-based radiofrequency SQUID is cooled to 4.2 K in LHe and is read out by a resonant LC circuit. The device is operated in feedback mode as a null detector of magnetic flux, and the small-signal bandwidth, slew rate, and noise of the flux-locked loop are characterized.

Introduction

Superconductivity is the result of a dissipative process (the scattering of an electron by a phonon) that, when taken to second order (the exchange of a virtual phonon between electrons), leads to the emergence of a new ground state with a reduced energy. The superconducting ground state can be described by a single quantum-mechanical wavefunction:

$$\Psi = \sqrt{\rho} e^{i\theta} \tag{1}$$

where ρ is a probability density, and θ is the phase of the superconducting wavefunction.

The single-valuedness of the superconducting wavefunction imposes the following quantization condition on the line integral of the vector potential **A** around a closed contour within the superconductor:

$$\Phi_T = \oint \vec{A} \cdot d\vec{s} = \frac{\hbar}{2e} \oint \nabla\theta \cdot d\vec{s} = n\Phi_0 \tag{2}$$

where Φ_T is the total magnetic flux threading the loop, *n* is an integer, and where we have introduced the magnetic flux quantum $\Phi_0 = h/2e \approx 2.07 \times 10^{-15}$ T m^2.

Equation (2) states that the flux threading a superconducting ring is quantized in units of the magnetic flux quantum, Φ_0. When a superconducting ring is cooled through T_c in the presence of a magnetic field, a circulating supercurrent is established in the ring which ensures that the total flux threading the loop (the sum of the flux due to the externally applied field and the flux due to the supercurrent) is equal to an integral number of magnetic flux quanta Φ_0; even after the removal of the external field, a supercurrent will flow in the loop indefinitely to preserve the flux state of the superconducting loop.

The introduction of a weak link, or Josephson junction, into the superconducting loop raises the possibility of a flux slip – the tunneling of a single flux quantum into or out of the loop. This phenomenon is the basis of the Superconducting QUantum Interference Device, or SQUID, the most sensitive detector of magnetic flux available. The SQUID comes in two varieties: (1) The dc SQUID incorporates two Josephson junctions; the device is biased with a dc current and read out at low frequencies. The theory and operation of the dc SQUID are described in the write-up accompanying the high-T_c dc SQUID ("Mr. SQUID") component of this experiment. (2) The radiofrequency SQUID, or rf SQUID, incorporates a single Josephson junction; the device is biased with a radiofrequency current, and is read out at high frequencies. The theory and operation of the rf SQUID are described below.

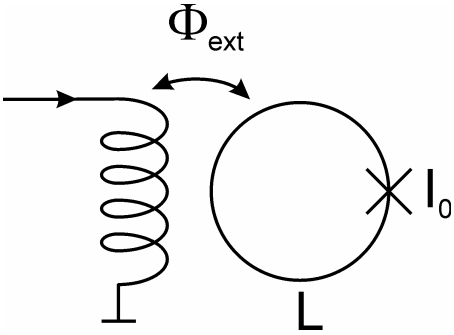

Figure 1. rf SQUID. The device consists of a superconducting loop of inductance L interrupted at one point by a Josephson junction with critical current I_0. The SQUID is biased with an external magnetic flux Φ_{ext}.

rf SQUID Theory

The rf SQUID is depicted schematically in Fig. 1. A superconducting loop of inductance L is interrupted at one point by a Josephson junction with critical current I_0. Since the Josephson junction can support a difference in phase δ in the superconducting wavefunction, the flux quantization condition in the SQUID reads

$$\delta + 2\pi \frac{\Phi_T}{\Phi_0} = 2\pi n. \tag{3}$$

From the dc Josephson relation, the supercurrent that flows through the junction is given by

$$I_{sc} = I_0 \sin\delta = -I_0 \sin\left(2\pi \frac{\Phi_T}{\Phi_0} \right). \tag{4}$$

At the same time, we can express the supercurrent in terms of fluxes and the loop inductance L, as follows:

$$I_{sc} = \frac{\Phi_T - \Phi_{ext}}{L}, \tag{5}$$

where Φ_{ext} is the flux due to the externally applied magnetic field. The flux state of the SQUID can be determined from the graphical construction of Fig. 2, where we plot both the Josephson current and the current through the loop inductance as a function of the

total flux Φ_T through the loop. The inductance of a circuit element can be determined from its current-flux characteristic, as follows:

$$L_{eff}(\Phi') = \left(\frac{\partial I}{\partial \Phi} \right)^{-1} \Bigg|_{\Phi'}, \tag{6}$$

where we have allowed for the possibility that the inductance of the circuit element under consideration varies as the flux is changed. Thus, the current-flux characteristic of the linear loop inductance of the SQUID is a straight line; on the other hand, the effective inductance of the Josephson junction is highly nonlinear. Indeed, the effective inductance L_J of the junction can be written as follows:

$$L_J = \frac{\Phi_0}{2\pi I_0 \cos\delta}. \tag{7}$$

Note that when the junction is biased with a current close to its critical current I_0, the phase difference δ across the junction goes to $\pi/2$ and the effective inductance of the junction diverges.

Returning to the graphical construction of Fig. 2, we note that the current through the Josephson junction must equal the current through the loop inductance; thus, the intersection points of the two current-flux characteristics determine the stable flux states of the loop. As the external flux bias Φ_{ext} is increased, the I-Φ characteristic of the inductor shifts vertically, moving the intersection point(s) and resulting in a change in the total flux Φ_T in the SQUID loop. As the junction critical current increases, the amplitude of the sine function increases, and thus the number of intersection points – and the number of possible flux states – increases. Finally, as the loop inductance L increases, the current-flux characteristic of the inductor becomes shallower, and the number of possible flux states increases. We introduce the reduced inductance

$$\beta_L \equiv \frac{2\pi I_0 L}{\Phi_0}, \tag{8}$$

which uniquely determines the quasistatic behavior of the rf SQUID. For $\beta_L > 1$, there exist flux biases for which the SQUID can exist in two (or more) stable flux states.

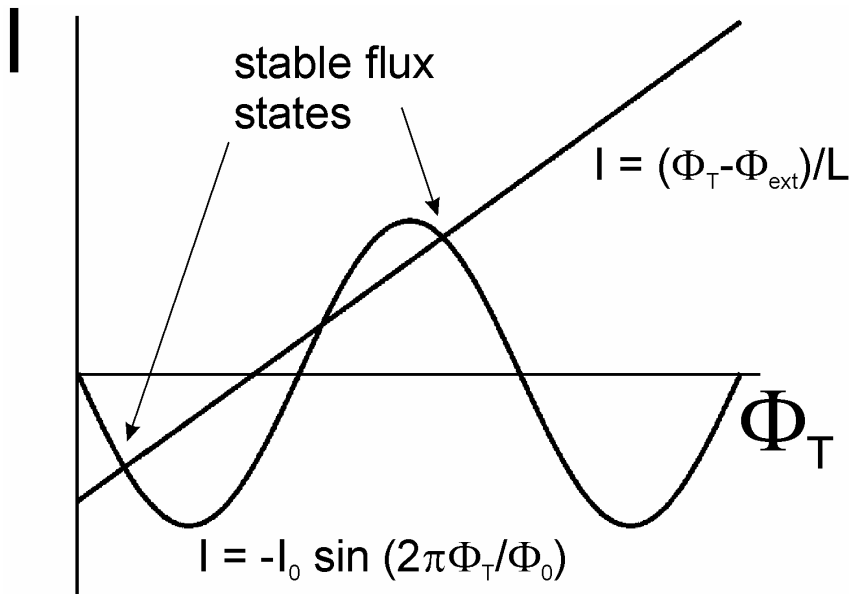

Figure 2. Current-flux characteristics for the loop inductance and Josephson junction of the rf SQUID.

In Fig. 3 we plot the total flux in the SQUID loop,

$$\Phi_T = \Phi_{ext} - LI_0 \sin\left(2\pi \frac{\Phi_T}{\Phi_0}\right), \tag{9}$$

as a function of the external flux Φ_{ext} for β_L= 7.9 (a typical value). Assume that the SQUID is initialized in the n=0 flux quantum state, with no applied flux (Φ_{ext}=Φ_T=0). We now increase the external flux. A circulating supercurrent is established which opposes the change in applied flux. As the applied flux is increased further, the circulating current eventually reaches the junction critical critical current (at an applied flux Φ_{ext}=Φ_C); at this point, the SQUID makes a transition from the n=0 flux state to the n=1 state. When the applied flux is now decreased, the SQUID remains in the n=1 flux state, until the applied flux reaches the (negative) value $2\Phi_C$-Φ_0, at which point it transitions to the n=0 flux state. The traversal of this hysteresis loop has dissipated an energy of the order of $I_0\Phi_0$.

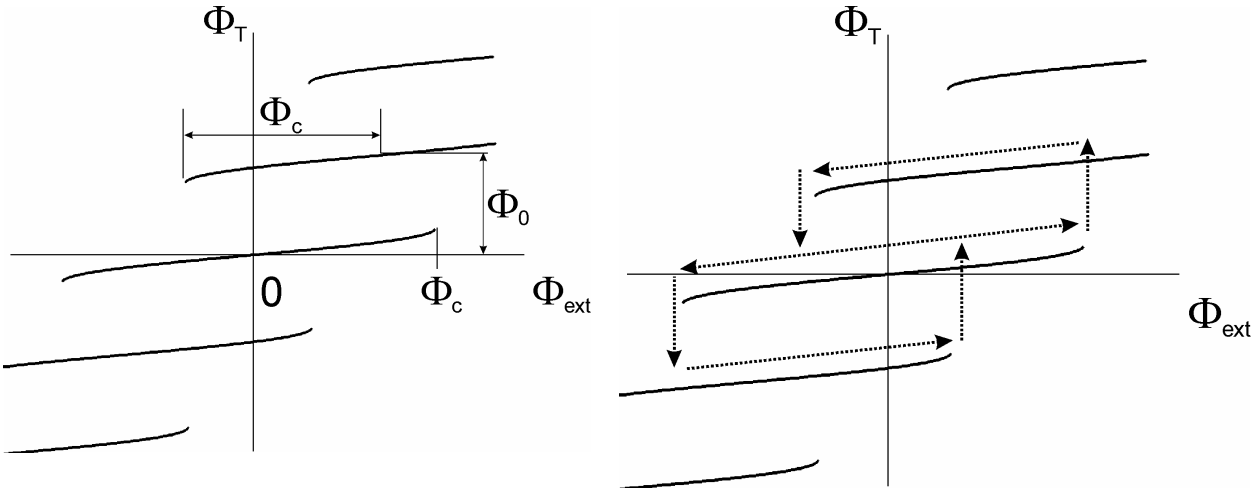

Figure 3. Total flux Φ_T versus applied external flux Φ_{ext} in an rf SQUID with β_L=7.9. (A) shows the critical flux Φ_C at which the induced supercurrent in the SQUID loop reaches the junction critical current I_0. (B) depicts the hysteresis loops that are traversed as an alternating external flux induces transitions between flux states.

rf SQUID Operation

In order to operate the rf SQUID as a sensitive detector of magnetic flux, the SQUID is inductively coupled to an LC tank circuit that is driven by a rf current $I_{rf} \sin \omega_0 t$ at the resonant frequency ω_0=1/sqrt(LC) of the tank (Fig. 4); typically $\omega_0/2\pi$ is in the range from tens to hundreds of MHz. The rf bias to the tank causes a current of amplitude $I_L = QI_{rf}$ to flow in the inductor of the tank circuit, where $Q = R/\omega_0 L$ is the quality factor of the tank circuit; this current in turn produces an rf flux bias at the SQUID, via a mutual inductance M. As the rf bias is increased from zero, the rf voltage V_{rf} across the tank circuit increases linearly with I_{rf} (Fig. 5). However, as soon as the alternating flux at the SQUID attains the value Φ_C, the SQUID traverses a hysteresis loop, moving from the n=0 flux state to either the n = +1 or n = -1 flux state and back to the n=0 state; when this occurs, the SQUID extracts an energy ~ $I_0\Phi_0$ from the tank circuit. For a relatively high tank Q, many rf cycles are required for the current in the tank circuit to recover to the point where the SQUID can undergo another flux transition. As the rf bias current is increased further, the SQUID continues to extract energy from the tank, but the tank circuit recovers more quickly as energy is supplied at a higher rate. For a broad range of rf bias current I_{rf}, the voltage across the tank circuit is independent of I_{rf}. Eventually rf energy is supplied to the tank circuit at such a rate that the SQUID undergoes a flux transition during every cycle of the rf drive, at which point the rf voltage across the tanks circuit begins once again to increase with increasing rf current drive. When the rf drive attains an amplitude that allows the SQUID to undergo transitions to the n = +2 or n = -2 flux states, another plateau appears in the V_{rf} versus I_{rf} curve.

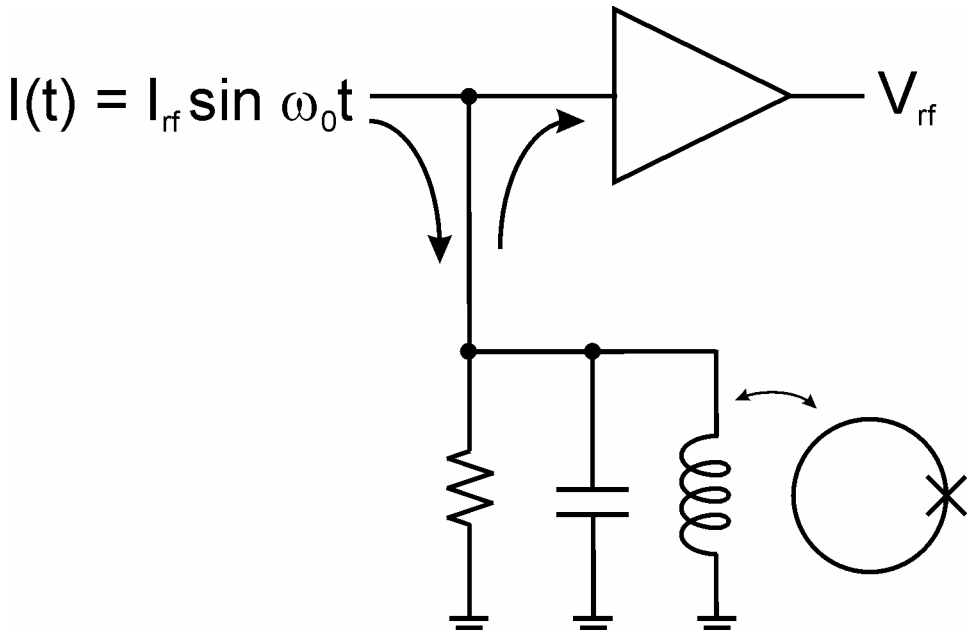

Figure 4. rf SQUID readout with a tuned LC circuit.

A shift in the quasistatic flux bias of the SQUID away from $\Phi=0$ causes flux transitions to occur at a reduced value of the rf bias I_{rf}. Fig. 5 displays the V_{rf} versus I_{rf} for quasistatic flux bias $\Phi_{ext}=n\Phi_0$ and for $\Phi_{ext}=(n+1/2)\Phi_0$, where n is an integer. The staircase pattern for bias at a half-integer number of flux quanta interlaces the staircase pattern for bias at an integer number of flux quanta. We see that when the tank circuit is biased at an rf current amplitude slightly above Φ_C/QM, the rf voltage across the tank circuit depends quite sensitively on the flux applied to the SQUID loop. A plot of the rf tank voltage versus applied flux reveals a triangle pattern, similar to that shown in Fig. 6. The rf voltage across the tank oscillates as a function of applied flux, with period equal to the magnetic flux quantum Φ_0.

We see from Fig. 6 that when the SQUID is biased with a magnetic flux $\Phi_{ext} \sim (2n+1)\Phi_0/4$, the rf voltage across the tank circuit is nearly proportional to small flux changes $\delta\Phi << \Phi_0$ applied to the SQUID loop; for small flux changes, the SQUID acts as a flux-to-voltage transducer. For large flux changes $\delta\Phi >> \Phi_0$, however, the rf voltage across the tank circuit is no longer proportional to the applied flux, due to the highly nonlinear nature of the flux-to-voltage transfer characteristic of the SQUID. This situation can be remedied, however, by operating the SQUID in a feedback loop, and using the device as a null detector of magnetic flux.

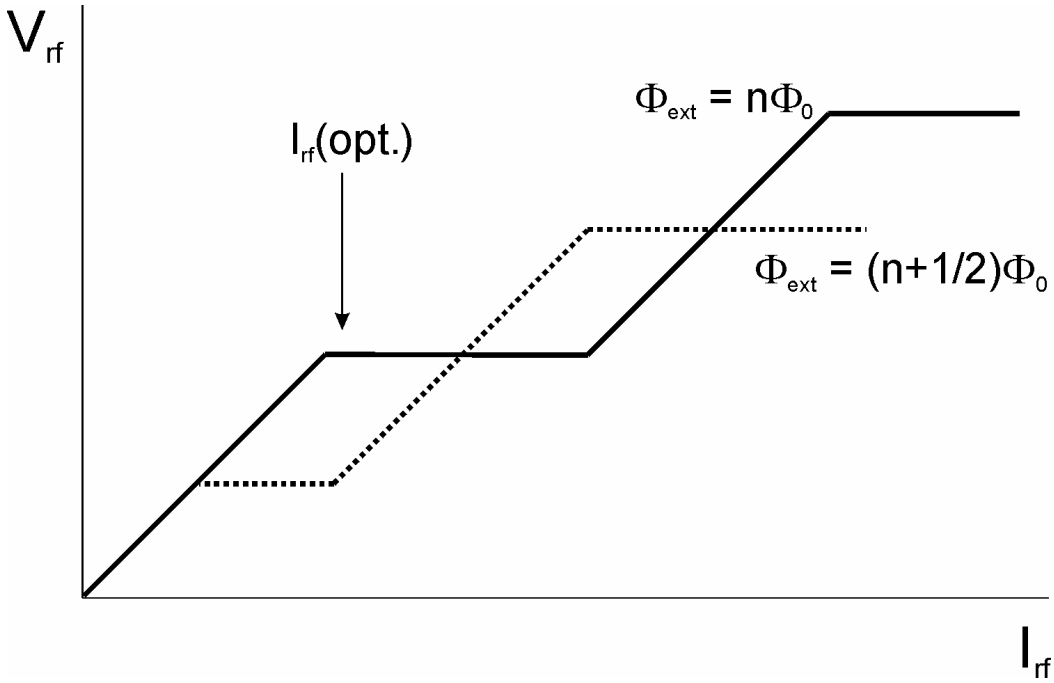

Figure 5. rf voltage across a tank circuit inductively coupled to an rf SQUID, as a function of rf current amplitude applied to the tank circuit, for integer and half-integer number of flux quanta applied to the rf SQUID. The arrow indicates the rf current bias that optimizes sensitivity of the SQUID to applied flux.

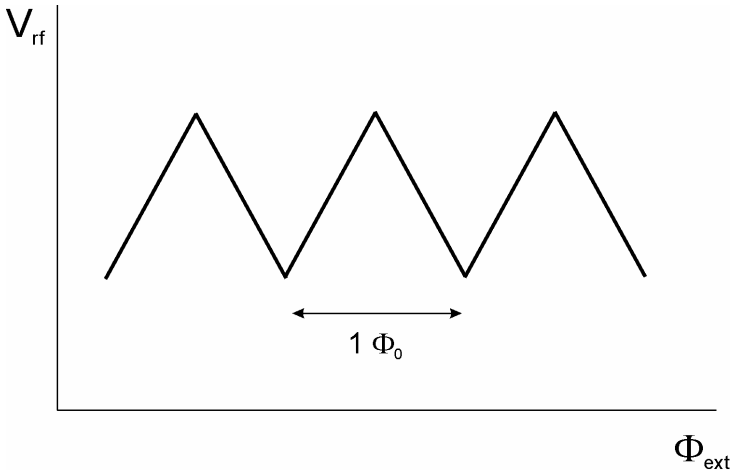

Figure 6. rf voltage across a tank circuit inductively coupled to an rf SQUID, as a function of the external flux applied to the SQUID.

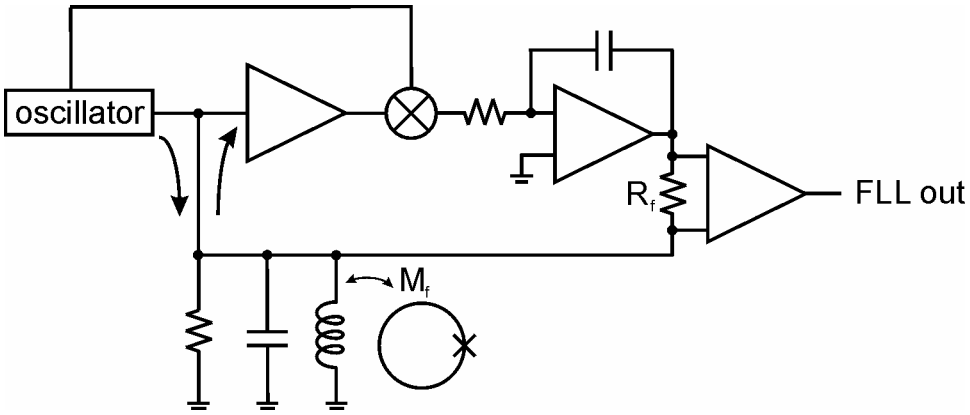

Figure 7. Block diagram of a flux-locked loop.

Flux-locked Loop

In this scheme, the rf voltage across the tank circuit is mixed down to dc, amplified, integrated, and fed back to the SQUID as a flux via a mutual inductance (typically the same that is used to provide the rf flux bias); a crude block diagram of a flux-locked loop is shown in Fig. 7. Here, feedback ensures that the quasistatic flux through the SQUID is unchanged as the external flux bias varies over many Φ_0, and that the SQUID remains optimally flux-biased at the steepest part of the flux-to-voltage transfer curve. The voltage drop across the feedback resistor R_f is now proportional to the applied flux.

In a further refinement, the quasistatic flux bias to the SQUID is modulated at a relatively low frequency of the order of 100 kHz, and lock-in detection is performed at this modulation frequency; for optimal sensitivity, the peak-to-peak amplitude of the flux modulation is adjusted to be $\Phi_0/2$. (This low frequency flux modulation does not replace, and is not to be confused with, the radiofrequency flux bias of the device, which is essential to rf SQUID operation). Advantages of this flux modulation scheme include a reduced sensitivity to low-frequency fluctuations of the critical current of the rf SQUID junction, which produce low-frequency noise in the SQUID flux-to-voltage transfer characteristic, and a reduced sensitivity to low-frequency 1/f noise in the room temperature electronics used to read out the device (however, while flux modulation eliminates 1/f critical current noise in an rf SQUID, it does NOT eliminate 1/f critical current noise in a dc SQUID; this is a somewhat subtle point). For a well designed SQUID readout system, one can achieve a slew rate in excess of 10^6 Φ_0/s, and detection sensitivity of the order of 1 $\mu\Phi_0$ in a 1 Hz bandwidth.

References

1. Giffard, R.P., Webb, R.A., and Wheatley, J.C., "Principles and Methods of Low-Frequency Electric and Magnetic Measurements Using an rf-Biased Point-Contact Superconducting Device", *J. Low Temp. Phys.* **6**, 533 (1972).
2. Van Duzer, T. and Turner, C.W., *Principles of Superconductive Devices and Circuits*, Elsevier, New York (1981).
3. Tinkham, M., *Introduction to Superconductivity*, McGraw-Hill, New York (1996).
4. Kittel, C., *Introduction to Solid State Physics*, Chapter 12, "Superconductivity", Wiley, New York (1986)

Apparatus

1. Liquid helium storage dewar.

2. Biomagnetic Technologies, Inc. (BTi) cryogenic dip probe, including niobium-based rf SQUID, tank circuit, high-frequency wiring, and niobium superconducting shield.

3. BTi preamplifier module (mounts directly on top of the dip probe).

4. BTi SQUID control box.

5. Tektronix digital oscilloscope.

6. Wavetek function generator.

7. Stanford Research Systems 560 low-noise preamplifier.

8. Keithley Instruments digital multimeter.

Procedures

1. Connect the rf SQUID preamplifier module to the rf SQUID probe head, and connect the cable from the preamplifier module to the SQUID control box. Tune the resonance frequency of the tank circuit to the frequency of the rf drive using the procedure outlined in the BTi rf SQUID operating manual.

2. SLOWLY lower the rf SQUID probe into the LHe storage dewar. By lowering the probe slowly you take advantage of the considerable enthalpy of the cold helium gas to cool the probe, and minimize the consumption of LHe. Use a foam plug to cover the mouth of the storage dewar. This minimizes cryopumping of air, which leads to the accumulation of liquid oxygen in the dewar (this is an explosion hazard).

3. Switch the SQUID control box to mode 1. In this mode, a low frequency (~100 Hz) test signal with a peak-to-peak amplitude of approximately 8 Φ_0 is applied to the SQUID. Display the output of the rf detector on an oscilloscope. Adjust the magnitude of the rf drive current to maximize the peak-to-peak voltage swing at the detector output. You are now biased at the first constant voltage step, as described in the discussion of Fig. 5 above. Make sure you understand the frequency multiplication of the triangle waveform that occurs when the SQUID is swept through many flux quanta. Digitize and print out the detector waveform. Notice that the voltage output of the detector decreases as the bias power is increased past the first constant voltage step. Increase the bias power until you

reach the second constant voltage step. What is the detector output at this point? Reduce the rf bias so that you are again operating at the first constant voltage step. Adjust the offset potentiometer at the front of the SQUID control box; this adds a dc offset flux to the SQUID loop. Explain what happens to the waveform at the detector output.

4. Switch the SQUID control box to mode 2. In this mode an intermediate frequency (~100 kHz) square-wave modulation signal is applied to the SQUID, in addition to the low-frequency test signal. You will perform a lock-in detection of the SQUID signal at this modulation frequency. Observe the detector output on the oscilloscope as you increase the modulation amplitude. Describe what you see. Adjust the modulation amplitude to the optimal peak-to-peak value of $\Phi_0/2$.

5. Operate the SQUID in the flux-locked loop, and display the output of the loop on the oscilloscope. Apply an offset flux to the SQUID to move the loop output away from 0 volts, and then reset the loop to cause the SQUID flux state to "slip" by an integer number of flux quanta. Repeat this several times, each time recording the magnitude of the voltage jump. From these measurements you will be able to refer the voltage at the flux-locked loop output to the flux applied to the SQUID. Note that the flux-to-voltage transfer function of the flux-locked loop has nothing to do with the flux-to-voltage transfer function of the SQUID itself, and is determined solely by the component values used in the feedback loop. In fact , the voltage change V at the loop output for a flux change Φ_0 applied to the SQUID loop is given by $V = \Phi_0(R_f/M_f)$, where R_f is the feedback resistance and M_f is the mutual inductance of the feedback coil to the SQUID. Be sure you can explain where this relation comes from.

6. Connect a function generator to the TEST input at the back of the SQUID control box, and apply a small-amplitude sinusoidal signal to the SQUID. Increase the frequency of this test signal and observe the flux-locked loop output to measure the small-signal bandwidth of the flux-locked loop. How is the loop bandwidth affected when you increase or decrease the rf bias from the optimal point?

7. Decrease the frequency of the test signal to a value that is far below the small-signal bandwidth of the flux-locked loop. Now increase the amplitude of the signal until the loop starts to become unstable. Record the slew rate of the flux-locked loop, expressing it in Φ_0/s.

8. Now disconnect the test signal and reset the flux-locked loop so that the loop output is near 0 volts. Use the Stanford Research Systems 560 to bandpass filter the output of the flux-locked loop, and measure the rms voltage noise over this band with the Keithley Instruments digital voltmeter. You should implement the internal 60 Hz notch to remove line interference from the flux-locked loop output. From the known bandwidth of the bandpass filter and from previous measurements, the rms voltage noise can be referred to a spectral density of flux noise at the input to the SQUID. Does the noise you measure agree with the value given in the BTi manual? What is the physical origin of this noise?